

Acute Hepatotoxicity: A Predictive Model Based on Focused Illumina Microarrays

Nadine Zidek,* Juergen Hellmann,† Peter-Juergen Kramer,‡ and Philip G. Hewitt*¹

*Molecular Toxicology, †Pathology and Histopathology, and ‡Institute of Toxicology, Merck KGaA, Darmstadt, 64293 Germany

Received February 28, 2007; accepted May 14, 2007

Drug-induced hepatotoxicity is a major issue for drug development, and toxicogenomics has the potential to predict toxicity during early toxicity screening. A bead-based Illumina oligonucleotide microarray containing 550 liver specific genes has been developed. We have established a predictive screening system for acute hepatotoxicity by analyzing differential gene expression profiles of well-known hepatotoxic and nonhepatotoxic compounds. Low and high doses of tetracycline, carbon tetrachloride (CCL₄), 1-naphthylisothiocyanate (ANIT), erythromycin estolate, acetaminophen (AAP), or chloroform as hepatotoxicants, clofibrate, theophylline, naloxone, estradiol, quinidine, or dexamethasone as nonhepatotoxic compounds, were administered as a single dose to male Sprague–Dawley rats. After 6, 24, and 72 h, livers were taken for histopathological evaluation and for analysis of gene expression alterations. All hepatotoxic compounds tested generated individual gene expression profiles. Based on leave-one-out cross-validation analysis, gene expression profiling allowed the accurate discrimination of all model compounds, 24 h after high dose treatment. Even during the regeneration phase, 72 h after treatment, CCL₄, ANIT, and AAP were predicted to be hepatotoxic, and only these three compounds showed histopathological changes at this time. Furthermore, we identified 64 potential marker genes responsible for class prediction, which reflected typical hepatotoxicity responses. These genes and pathways, commonly deregulated by hepatotoxicants, may be indicative of the early characterization of hepatotoxicity and possibly predictive of later hepatotoxicity onset. Two unknown test compounds were used for prevalidating the screening test system, with both being correctly predicted. We conclude that focused gene microarrays are sufficient to classify compounds with respect to toxicity prediction.

Key Words: gene expression changes; toxicogenomics; early prediction; screening model; Illumina microarray; rat *in vivo* model.

Toxicology testing is central for the safety of drug development candidates. Indeed, adverse drug effects are still a major reason for drug withdrawal from the market. Hence, new powerful techniques are needed to improve the detection

of potentially toxic compounds from the drug development process earlier. Toxicogenomics, which makes use of DNA microarray technologies and measures the expression of thousands of genes simultaneously, has the potential to revolutionize toxicology. It has been used as a tool to elucidate mechanisms and to predict toxicity (Duggan *et al.*, 1999; Hamadeh *et al.*, 2002). The advanced knowledge of gene expression patterns together with modern classification algorithms has demonstrated practical benefits for predicting pathological events and toxic endpoints (Steiner *et al.*, 2004; Waring *et al.*, 2001). Thus, this gain of information can potentially reduce the duration of preclinical toxicology studies and consequently the number of animals needed. Additionally, regulatory agencies are encouraging the use of modern molecular techniques, such as animal or computer-based predictive models and safety biomarkers, to improve predictability and efficiency from laboratory concept to commercial product. In fact, the Food and Drug Administration recognizes the importance in pharmacogenomics and encourages its use in drug development and has released guidance documents for submission (<http://www.fda.gov/cder/genomics/>).

Predictive toxicology relies mainly on class prediction, whose methods are based on the assumption that gene expression profiles of known toxins from representative toxicological classes (model compounds) can predict the toxicological effects of unknown compounds (UNCs) based on similarities between gene expression profiles (Maggioli *et al.*, 2006; Schena *et al.*, 1995). Thus, gene expression data can provide an early indication of toxicity because toxin-mediated changes in gene expression are often detectable before clinical chemistry, histopathology, or clinical observations (Ulrich and Friend, 2002).

Thomas *et al.* (2001) published one of the first classification algorithms used for the accurate prediction of 24 model compounds based on leave-one-out cross-validation of a large microarray database. Hamadeh *et al.* (2002) used discrimination algorithms to classify blind samples based on a training set using high-density gene expression profiles. Steiner *et al.* (2004) used support vector machine (SVM) to obtain an optimal discrimination between hepatotoxic and nonhepatotoxic compounds (based on 26 toxic compounds) with their whole genome

¹ To whom correspondence should be addressed at Institute of Toxicology – Molecular Toxicology, Merck KGaA, Frankfurter Str. 250, 64293 Darmstadt, Germany. Fax: +49-6151-912927. E-mail: philip.hewitt@merck.de.

Affymetrix microarray profiles. These studies varied in experimental design (e.g., time of dosage and number of compounds investigated), but all indicated the potential of toxicogenomics in predictive toxicological risk assessment.

Due to the demand for cheaper, higher-throughput screening systems for toxicity testing, as well as the relatively high costs of high density arrays, the question arises whether a microarray focused on toxicologically relevant genes could also be predictive. Therefore, we established an oligonucleotide microarray with 550 genes, chosen based on their known involvement in hepatotoxicity (published information and internal Merck KGaA bioinformatic data from previous studies), to aid in the classification and risk assessment of acute hepatotoxicity. Our customized focused microarray was designed using the oligonucleotide Sentrix BeadChips (Illumina, Inc., San Diego, CA) based on the BeadArray technology (Gunderson *et al.*, 2004; Steemers and Gunderson, 2005).

Due to the fact that the liver is the primary site for drug metabolism and hepatotoxicity is one of the most frequently reported human adverse drug reactions, we concentrated on the prediction of hepatotoxicity. Thus, 12 model compounds, including six well-known hepatotoxicants, were chosen based on an extensive literature study, namely carbon tetrachloride (CCL₄), chloroform (CHCL₃), both inducers of necrosis and steatosis (Brattin *et al.*, 1985; Minami *et al.*, 2005; Wang *et al.*, 1997; Weber *et al.*, 2003; Yamamoto *et al.*, 2006), 1-naphthylisothiocyanate (ANIT) a well-known cholestasis inducer (Krell *et al.*, 1982; Mehendale *et al.*, 1994; Orsler *et al.*, 1999), the antibiotics tetracycline (TET), and erythromycin estolate (EE) which cause steatosis and cholestasis, respectively (Amacher and Martin 1997; de Longueville *et al.*, 2003; Fromenty and Pessayre, 1995; Garcia Monzon *et al.*, 1985; Venkateswaran *et al.*, 1998; Yamamoto *et al.*, 2006), and the drug acetaminophen (AAP), a well-known hepatotoxicant causing liver necrosis (James *et al.*, 2003; Minami *et al.*, 2005; Prescott, 1980; Yamamoto *et al.*, 2006). As nonacute rodent hepatotoxicants the drugs clofibrate (CF) (peroxisome proliferator-activated receptor [PPAR- α] agonist) (Corton *et al.*, 2000; Richert *et al.*, 2003; Yadetie *et al.*, 2003), theophylline (THEO) (diuretic), naloxone (NLX) (analgesic), estradiol (E2) (estrogen), quinidine (QUIN) (antiarrhythmic), and dexamethasone (DEX) (corticosteroid) were chosen.

The primary goal of the current paper was to determine whether gene expression based on a relative small set of genes could discriminate between animals acutely treated with various model compounds known to cause hepatotoxicity or with nonhepatotoxic compounds at different time points and dose levels. Such a discriminatory model maybe used for the early characterization of potential hepatotoxicants and maybe for the prediction of chronic hepatotoxic endpoints. Above all, in respect to the 3Rs concept, this would mean significant reduction in animal usage due to the performance of shorter-term studies for the early classification of novel untested compounds.

MATERIALS AND METHODS

Animal Treatment

Tissue samples, used for transcription profiling, were derived from studies using albino Sprague–Dawley rats (CrI:CD) treated by single intraperitoneal injection with test compounds and were obtained from an external tissue bank (PHASE-1 Santa Fe, NM). All studies were performed according to Good Laboratory Praxis (GLP). Briefly, male Sprague–Dawley rats approximately 10–11 weeks old were maintained on certified rodent chow (PMI Feeds Inc., Purina Mills, Richmond, IN) and tap water *ad libitum* in individual stainless steel cages at a 12-h light/12-h dark period. Treatment was conducted at two dose levels: (1) a maximum tolerated dose (MTD) level (high dose [hd]), which was chosen based on clear signs of toxicity with little or no lethality (published and unpublished information) and (2) around ¼ of the MTD level (low dose [ld]). The following test compounds were chosen: TET 50 mg/kg (ld) or 150 mg/kg (hd), ANIT 15 mg/kg (ld) or 60 mg/kg (hd), THEO 25 mg/kg (ld) or 100 mg/kg (hd), NLX 45 mg/kg (ld) or 180 mg/kg (hd), QUIN 25 mg/kg (ld) or 100 mg/kg (hd), DEX 8 mg/kg (ld) or 30 mg/kg (hd), CHCL₃ 0.25 ml/kg (hd) (all prepared in saline), CCL₄ 0.25 ml/kg (ld) or 1 ml/kg (hd), CHCL₃ 0.1 ml/kg (ld) (both prepared in corn oil), EE 40 mg/kg (ld) or 160 mg/kg (hd), CF 75 mg/kg (ld), or 250 mg/kg (hd) (both prepared in 8%polyethylene glycol/8% ETOH), E2 0.1 mg/kg (ld) or 0.4 mg/kg (hd) (prepared in 5% ETOH), or AAP 250 mg/kg (ld) or 1000 mg/kg (hd) (prepared in water). Control groups were treated with vehicle only. Three rats were used for each treatment, control group or time point, and sacrificed at 6, 24, or 72 h. Livers were taken for histopathological evaluation (by PHASE 1 Molecular Toxicology, Inc.) and remaining liver tissues were snap frozen in liquid nitrogen, stored at – 80°C, and transferred to our laboratory for further analysis.

Histopathology

Histopathological examinations of the liver section from all animals of the 72-h groups, stained with hematoxylin and eosin, were conducted by PHASE 1, Inc. The observed liver alterations were scored and categorized (Table 2).

RNA Isolation and Analysis

Total RNA from liver samples (50–90 mg) was isolated using TRI REAGENT (Sigma-Aldrich Inc., St Louis, MO) according to the manufacture's instruction. In addition, after the ethanol precipitation step in the extraction procedure, a cleanup step using the QIAGEN RNeasy Mini kit columns (Qiagen GmbH, Hilden, Germany) was performed to obtain a better yield for later *in vitro* transcription labeling. The quality of total RNA was checked by gel analysis using the total RNA Nano chip assay on an Agilent 2100 Bioanalyzer (Agilent Technologies GmbH, Berlin, Germany). RNA concentrations were determined using the NanoDrop spectrophotometer (NanoDrop Technologies, Wilmington, DE).

Probe Labeling and Illumina Sentrix BeadChip array Hybridization

Biotin-labeled cRNA samples for hybridization on custom Illumina Sentrix BeadChip arrays (Illumina, Inc.) were prepared according to Illumina's recommended sample labeling procedure based on the modified Eberwine protocol (Eberwine *et al.*, 1992). In brief, 500 ng total RNA was used for complementary DNA (cDNA) synthesis, followed by an amplification/labeling step (*in vitro* transcription) to synthesize biotin-labeled cRNA according to the MessageAmp II aRNA Amplification kit (Ambion, Inc., Austin, TX), with the following modifications requested by Illumina: standard reactions were cut down to ¼ size, separate annealing step of the T7 oligo(dT) primer was omitted (single step of the first-strand cDNA synthesis), and cleanup columns were replaced. QIAquick PCR Purification kit and QIAGEN RNeasy Mini kit (Qiagen), used according to the manufacture's recommendations, were used for cDNA purification (elution with water instead of the kits EB buffer) and for cRNA purification (eluted two times with 50 μ l of water), respectively. Biotin-16-UTP was purchased from PerkinElmer Life and Analytical Sciences, Boston, MA. Due to a reduced amount of standard reactions, total RNA and purified

cDNA were dried down and then dissolved in synthesis solutions. The column-purified cRNA was quality controlled using the messenger RNA (mRNA) Nano Chip Assay on an Agilent 2100 Bioanalyzer and spectrophotometrically quantified (NanoDrop).

Five hundred nanograms of amplified biotin-labeled cRNA was then prepared in a solution of 45% (vol/vol) Hyb E1 buffer (Illumina, Inc.) and 25% (vol/vol) deionized formamide (Ambion, Inc.) at a final concentration of 25 ng/ μ l. After preheating at 65°C for 5 min the cRNA samples were hybridized with the Sentrix BeadChips in a BeadChip Hyb Cartridge for 18 h at 55°C (Hybaid Maxi 14 hybridization oven, Thermo Electron Corporation, Waltham, MA). After hybridization, the Sentrix BeadChips were washed for 15 min on an orbital shaker in 250 ml of 0.3% (vol/vol) Wash E1BC buffer (Illumina, Inc.) solution and then blocked for 5 min in 4 ml of 1% (wt/vol) Blocker Casein in phosphate buffered saline, Hammarsten grade (Pierce Biotechnology, Inc., Rockford, IL). Array signals were developed by a 10-min incubation in 2 ml of 1 μ g/ml Cy3-streptavidin (Amersham Biosciences, Buckinghamshire, UK) solution and 1% blocking solution. The BeadChips were washed a second time in diluted Wash E1BC buffer for 5 min, dried immediately after removal by centrifugation at 275 \times g for 4 min at 25°C, and scanned.

Focused Illumina BeadChip microarray Analysis

Data acquisition. The focused Sentrix Illumina BeadChips, with each BeadChip comprising eight microarrays on a glass slide, were scanned at a wavelength of 532 nm and 5- μ m resolution on the GenePix 4000B Microarray Scanner (Axon Instruments Inc., Union City, CA; Molecular Devices Corporation, Sunnyvale, CA). Images were captured with the GenePix Pro 5.0 software (Axon, Molecular Devices Corporation) according to the manufacturer's instructions. Due to the random nature of the assembled microarrays all spots in the image were aligned with a de-code map (result of the manufacturers decoding process, delivered with each focused Illumina microarray) containing the positions of all 50,000 randomly assembled microbeads on the array and the identities of the probes found on those beads (Galinsky, 2003; Gunderson *et al.*, 2004). The decoding process, which uses a molecular address, is part of the array manufacture procedure and provides a quality control for all elements of every array (Gunderson *et al.*, 2004). Subsequently, bead signal intensity extraction, using the imaging and data extraction software, AnEx (Illumina, Inc.), was performed prior to further analysis. The focused Illumina microarrays contain about 1500 unique probe sequences (Probe ID), or bead types (two 50 mer oligonucleotide probes/gene), corresponding to 550 annotated rat genes and several control genes (Gene ID). Each probe sequence is represented by approximately 30 beads on each array and each bead contains more than 10⁵ copies of unique covalently attached oligonucleotide probes (Gunderson *et al.*, 2004; Steemers and Gunderson, 2005). Using AnEx, the intensities of all beads (~30) were condensed to an average intensity value per probe ID and then further condensed to one signal intensity value per Gene ID. This is associated with a detection *p* value calculated from the background, characterized by the chance that the target sequence signal was distinguishable from the negative controls. Gene IDs with detection values > 0.99 were designated as reliable.

Array quality. Focused Illumina microarray quality was determined by image viewing and incorporated control bead analysis (housekeeping, hybridization, signal generation, and background). Arrays with overall intensity outliers from the majority of arrays (caused by poor hybridization conditions or poor imaging) were excluded from further analysis. Fourteen housekeeping genes were used to check the intactness of the biological sample. Hybridization controls covering (1) three concentrations (low, medium, and high) of Cy3-labeled oligonucleotides present in the Hyb E1 buffer were used to yield a gradient hybridization response signal independent of both the cellular RNA quality and success of the sample preparation reactions (six probes), (2) Cy3-labeled probes, including a mismatch oligonucleotide with two single base changes (each), to control for nonspecific hybridization (four probes), and (3) Cy3-labeled oligonucleotide target with a high G-C content to check the stringency grade (one probe). Two probes with complementary biotin-tagged oligonucleotides present in the Hyb E1 buffer were used to control for signal

generation. Negative controls consisting of 20 probes of random sequences selected to have no corresponding targets in the rat genome were used to define a background signal, representing the image system background as well as any signal resulting from nonspecific binding of dye or cross-hybridization.

Normalization. Quality controlled focused Illumina microarrays were "chip-wise" normalized using the rank invariant algorithm (Kuhn *et al.*, 2004) and resulting data further analyzed using the Expressionist Analyst software (GeneData, Basel, Switzerland). Briefly, a second normalization of all microarrays over all gene signal intensities based on the arithmetic mean was performed. Comparative analysis between control and treated samples was done separately for each individual compound, including fold change (average signal intensity treated/average signal intensity control) and a significance value (*p* value), calculated using a two-tailed, unpaired *t*-test. A *p* value less than 0.05 was accepted as significant. In addition, the false discovery rate (FDR, Benjamini-Hochberg *q* value) was determined and included into Table 3 to improve the relevance of these significantly deregulated genes.

Modeling/classification. For SVM classification, implemented in the cross-validation tool of Expressionist Analyst software, only normalized intensity values of the treated samples were considered. The samples were categorized as either hepatotoxic or nonhepatotoxic and further subcategorized into the time and dose. A linear kernel and a penalty of 10 were chosen as the parameters for the SVM algorithm. The leave-one-out cross-validation scheme with 12 repeats (representing the number of compounds) was used for a robust discrimination. Genes for final discrimination between hepatotoxicity and nonhepatotoxicity were identified by gene ranking analysis of variance (ANOVA). Molecular functions of the genes were individually annotated by using the classification schemes in Gene Ontology, KEGG database (keg.org), and MetaCore 3.1 software (GeneGO, Inc., St Joseph, MI).

Real-time PCR

All RNA samples from the hd 24-h animals and their corresponding time-matched vehicle controls were used to verify 13 genes (Table 1) with different biological functions, chosen from the pool of discriminative genes. Since classification models for discrimination analysis do not primarily select either significant and/or genes with pronounced fold changes from either hepatotoxicants or nonhepatotoxic compounds as discriminative gene, the acute phase gene Metallothionein 1a (*Mt1a*) was added as it showed distinct deregulation by many of the compounds (similar to a positive control). Two housekeeping genes, 18S ribosomal RNA (rRNA) and *B2m*, were run in parallel.

cDNA synthesis and analysis. One microgram total RNA was reverse transcribed to cDNA using random hexamer primers with the first-strand cDNA synthesis kit for reverse transcription-PCR (RT-PCR) avian myeloblastosis virus reverse transcriptase (Roche, Mannheim, Germany) according to the manufacturer's instructions. The quality and quantity of cDNA was determined using the Agilent Bioanalyzer 2100 together with the mRNA Pico Assay (Agilent Technologies, Waldbronn, Germany) according to the manufacturer's instructions.

TaqMan low density array. Real-time PCR analysis was performed using TaqMan Low Density Arrays (Applied Biosystems, Darmstadt, Germany). Real-time PCR primers and probes ("TaqMan Gene Expression Assays") for the rat genes listed in Table 1 were spotted onto a 384-well card (TaqMan Low Density Array). Eight samples were analyzed per card. Each sample was measured in triplicate in a single RT-PCR run. Five nanograms of single strand cDNA, mixed with qPCR Mastermix Plus (Eurogentec, Seraing, Belgium), in a total volume of 100 μ l, was loaded per sample loading port. Thermal cycling and fluorescence detection were performed on Applied Biosystems ABI Prism 7900HT Sequence Detection System with ABI Prism 7900HT SDS Software 2.1. Forty-five cycles were run with the following parameters: 2 min at 50°C, 10 min at 94.5°C, and for each cycle 30 s at 97°C for denaturation and 1 min at 59.7°C for transcription. Analysis of gene expression values was performed using the efficiency-corrected comparative *C_T* (threshold-cycle) method, determining target gene expression relative to either 18S rRNA or *B2m* endogenous control expression and relative to the control sample. Real-time

TABLE 1
Genes Present on the TaqMan LowDensity Array with their Respective TaqMan Gene Expression Assay Numbers and RefSeq Numbers

Gene symbol	Gene name	TaqMan gene expression assay number	RefSeq number
<i>Abcb1</i>	ATP-binding cassette, subfamily B (MDR/TAP), member 1	Rn00561753_m1	NM_012623
<i>Acly</i>	ATP citrate lyase	Rn00566411_m1	NM_016987
<i>B2m</i>	beta-2 Microglobulin	Rn00560865_m1	NM_012512
<i>Cat</i>	Catalase	Rn00560930_m1	NM_012520
<i>Fmo1</i>	Flavin containing monooxygenase 1	Rn00562945_m1	NM_012792
<i>Gadd45a</i>	Growth arrest and DNA damage-inducible 45 alpha	Rn00577049_m1	NM_024127
<i>Gstm3</i>	Glutathione S-transferase, mu type 3	Rn00579867_m1	NM_031154
<i>Igfbp1</i>	Insulin-like growth factor binding protein 1	Rn00565713_m1	NM_013144
<i>Lbp</i>	Lipopolysaccharide binding protein	Rn00567985_m1	NM_017208
<i>Mt1a</i>	Metallothionein	Rn00821759_g1	NM_138826
<i>Otc</i>	Ornithine transcarbamylase	Rn00565169_m1	NM_013078
<i>Pygl</i>	Liver glycogen phosphorylase	Rn00573974_m1	NM_022268
<i>S100a9</i>	S100 calcium binding protein A9 (calgranulin B)	Rn00585879_m1	NM_053587
<i>Stat3</i>	Signal transducer and activator of transcription 3	Rn00562562_m1	NM_012747
<i>Timp1</i>	Tissue inhibitor of metalloproteinase 1	Rn00587558_m1	NM_053819

PCR efficiencies for the above mentioned assays were determined by performing the reaction with a dilution series of cDNA (100, 10, 1, and 0.1 ng per sample loading port) prepared from control rat liver total RNA. Efficiency values and gene expression ratios were calculated as previously described by Tuschl and Mueller (2006).

RESULTS

Animal Testing and Histopathology

After exposure to all nonhepatotoxicants as well as the UNC B, no histopathological alterations were found. On the other hand CCL4, ANIT, and AAP showed histopathological changes 72 h after treatment. CCL4 showed mild liver cell necrosis at 1d that increased to severe liver cell damage combined with secondary inflammatory and minimal regenerative/proliferative effects after hd administration. Histopathological changes of ANIT and AAP were restricted to hd exposure and consisted of minimal liver cell necrosis. In addition, ANIT showed minimal secondary inflammatory and regenerative effects as well as moderate bile duct hyperplasia. The UNC A showed minimal liver cell necrosis and inflammation at low level exposure and increased to moderate liver cell damage combined with mild secondary effects. Histopathology evaluation is summarized in Table 2.

Principal Component Analysis of Model Compounds

In order to detect acute hepatotoxic effects of model compounds on the gene expression level, total RNA from rat livers given a single ld or hd of compound was isolated 6, 24, and 72 h after administration.

The unsupervised method, principal component analysis (PCA), is suited to separate natural subpopulations in an

unbiased manner. To determine whether gene expression could separate samples treated with model hepatotoxic compounds at different time points and dose levels, PCA was used to visualize sample distribution. PCA analyses were conducted on all 550 genes on the microarray. Figure 1 shows all 12 compounds, including, time-matched vehicle controls (yellow), nonhepatotoxic (blue), and hepatotoxic compounds (others) 6, 24, and 72 h after hd treatment. Distinct separation of most hepatotoxicants, especially CCL4 and TET, into subclouds separated from the other experiments (including the time-matched vehicle controls and nonhepatotoxicants), was observed after 24 h. Experiments 6 h after low (data not shown) and hd treatment did not show distinguishable clusters, due to a high variability in the gene expression data. However, the hepatotoxicants ANIT and CCL4 were separated from the other experiments even 72 h after hd treatment. It is clear from Figure 1 that the TET experiments behaved differentially to the others (based on PCA). Even so, at 24-h TET treated animals showed a different gene expression than the corresponding vehicle control animals. By 72 h this was no longer the case.

Common Effects of Hepatotoxic Compounds

Gene expression profiles of all hepatotoxic and nonhepatotoxic compounds with a fold change deregulation of more than 1.5 and $p < 0.05$ were taken to find common significantly deregulated genes. Only for one condition, 24-h hd treatment, were five genes found to be deregulated by all six hepatotoxicants and not by nonhepatotoxicants (Table 3): ATP-binding cassette subfamily B (MDR/TAP) member 11, flavin containing monooxygenase (*Fmo1*), monoamine oxidase (*Maob*), liver glycogen phosphorylase (*Pygl*), and thioredoxin reductase (*Txnrd1*). The carbohydrate metabolism enzyme, *Pygl*, and

TABLE 2
Histopathological Findings at 72 h for All Compounds (Conducted by the Company PHASE 1, Inc.)

Compound	Compound symbol	Dose level	Necrosis	Inflammation	Regeneration/proliferation	Bile duct hyperplasia
Hepatotoxic compounds						
Acetaminophen	AAP	250 mg/kg (ld)	nad.	nad.	nad.	nad.
		1000 mg/kg (hd)	1	nad.	nad.	nad.
1-Naphthylisothiocyanate	ANIT	15 mg/kg (ld)	nad.	nad.	nad.	nad.
		60 mg/kg (hd)	1	1	1	3
Carbon tetrachloride	CCL4	0.25 ml/kg (ld)	2	nad.	nad.	nad.
		1 ml/kg (hd)	5	2	1	nad.
Chloroform	CHCL3	0.25 ml/kg (ld)	nad.	nad.	nad.	nad.
		0.5 ml/kg (hd)	nad.	nad.	nad.	nad.
Erythromycin estolate	EE	40 mg/kg (ld)	nad.	nad.	nad.	nad.
		160 mg/kg (hd)	nad.	nad.	nad.	nad.
Tetracycline	TET	50 mg/kg (ld)	nad.	nad.	nad.	nad.
		150 mg/kg (hd)	nad.	nad.	nad.	nad.
Nonhepatotoxic compounds						
Clofibrate	CF	75 mg/kg (ld)	nad.	nad.	nad.	nad.
		250 mg/kg (hd)	nad.	nad.	nad.	nad.
Dexamethasone	DEX	8 mg/kg (ld)	nad.	nad.	nad.	nad.
		30 mg/kg (hd)	nad.	nad.	nad.	nad.
Estradiol	E2	0.1 mg/kg (ld)	nad.	nad.	nad.	nad.
		0.4 mg/kg (hd)	nad.	nad.	nad.	nad.
Naloxone	NLX	45 ml/kg (ld)	nad.	nad.	nad.	nad.
		180 mg/kg (hd)	nad.	nad.	nad.	nad.
Quinidine	QUIN	25 mg/kg (ld)	nad.	nad.	nad.	nad.
		100 mg/kg (hd)	nad.	nad.	nad.	nad.
Theophylline	THEO	25 mg/kg (ld)	nad.	nad.	nad.	nad.
		100 mg/kg (hd)	nad.	nad.	nad.	nad.
UNCs						
Unknown compound A	UNC A	0.2 ml/kg (ld)	1	1	nad.	nad.
		0.8 ml/kg (hd)	3	2	1	nad.
Unknown compound B ^a	UNC B	ld	nad.	nad.	nad.	nad.
		hd	nad.	nad.	nad.	nad.

^aNotes. Findings after 24 h

Abbreviations: Severity Scoring: nad., nothing abnormal detected; 1, minimal; 2, mild; 3, moderate; 4, massive; 5, severe.

the xenobiotic metabolism Phase 1 enzymes, *Fmo1*, and *Maob*, were significantly downregulated by 2–3, 2–10, or 1.6–3 fold. *Abcb11*, which is involved in transporter activity, was signif-

icantly downregulated by all hepatotoxicants except for ANIT which showed significant diametrical regulation of 1.8-fold. The oxidative stress enzyme, *Txnrd1*, was significantly

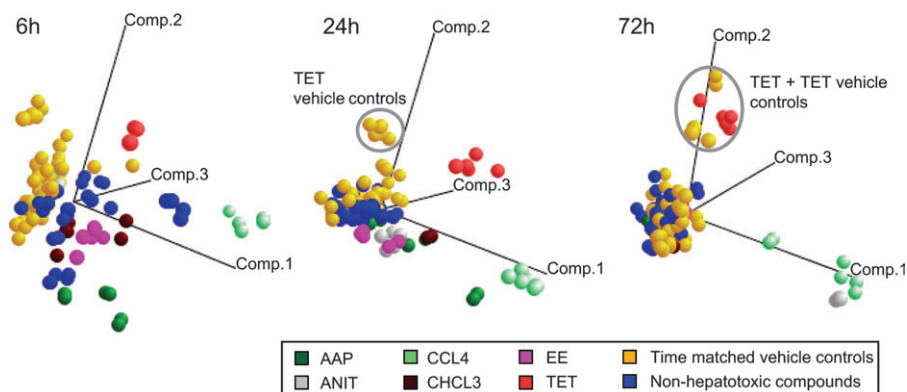


FIG. 1. PCA, a standard technique for visualization of complex data to get a first impression of the data distribution of each experiment and their global relationship/similarity to one another, shows all 12 compounds, including, time-matched vehicle controls (yellow), nonhepatotoxic (blue), and hepatotoxic compounds 6, 24, and 72 h after hd treatment.

TABLE 3
Common Genes Significantly Deregulated by all Hepatotoxicants but not by Nonhepatotoxicants after 24-h
hd Treatment (Fold Change 1.5 and $p < 0.05$)

Gene description	RefSeq	Symbol	Hepatotoxic compounds					
			TET	CCL4	ANIT	EE	AAP	CHCL3
Carbohydrate metabolism								
Liver glycogen phosphorylase	NM_022268	<i>Pygl</i>	-3.5 ⁺⁺⁺	-3.2 ⁺⁺⁺	-3.1 ⁺⁺	-2.5 ⁺⁺⁺	-3.2 ⁺⁺	-1.8 ⁺
Oxidative stress								
Thioredoxin reductase	NM_031614	<i>Txnrd1</i>	2.0 ⁺⁺⁺	2.6 ⁺⁺⁺	1.7 ⁺⁺⁺	-1.5 ⁺⁺	6.5 ⁺	2.3 ⁺⁺⁺
Xenobiotic metabolism/Phase 1								
Flavin containing monooxygenase 1	NM_012792	<i>Fmo1</i>	-2.9 ⁺⁺⁺	-10.7 ⁺⁺⁺	-3.9 ⁺⁺⁺	-2.0 ⁺⁺	-4.7 ⁺	-4.8 ⁺⁺⁺
Monoamine oxidase B	NM_013198	<i>Maob</i>	-1.6 ⁺⁺⁺	-3.2 ⁺⁺⁺	-1.7 ⁺⁺⁺	-1.9 ⁺⁺⁺	-1.8 ⁺	-1.6 ⁺⁺
Xenobiotic metabolism/Phase 3								
ATP-binding cassette, sub-family B (MDR/TAP), member 11 (synonym: bile salt export pump)	NM_031760	<i>Abcb11 (Bsep)</i>	-1.8 ⁺⁺⁺	-2.6 ⁺⁺⁺	1.8 ⁺⁺⁺	-1.5 ⁺	-3.1 ⁺⁺	-1.8 ⁺⁺

Note. The FDR of these genes are rated and marked with “+” for $q < 0.1$, “+++” for $q < 0.01$, “++++” for $q < 0.001$.

upregulated by hepatotoxic compounds except for EE, which showed a small but significant downregulation 24 h after hd treatment.

Discrimination between Hepatotoxic and Nonhepatotoxic Compounds

Leave-one-out cross-validation (via SVM) using all 550 genes was performed for all normalized treated samples from all 12 compounds to distinguish between hepatotoxic and nonhepatotoxic model compounds. In Figure 2, tile plots show that 6 h after hd administration several compounds were misclassified (misclassification rate 58.3%). However, 24 h after hd treatment gene expression profiles allowed the correct

classification of all compounds. After 72 h all nonhepatotoxic compounds were correctly predicted and three of the hepatotoxic compounds were predicted to be nonhepatotoxic (misclassification rate 25%). Only AAP, ANIT, and CCL4 were predicted to be hepatotoxic 72 h after administration. Gene expression profiles obtained from 1d administration of all 12 compounds were incorrectly predicted at all time point (misclassification rates of 66.7% [6 h], 50% [24 h], and 66.7% [72 h] were obtained).

Gene Ranking Analysis

The ANOVA ranking method analysis was used to achieve a gene set which was responsible for the correct

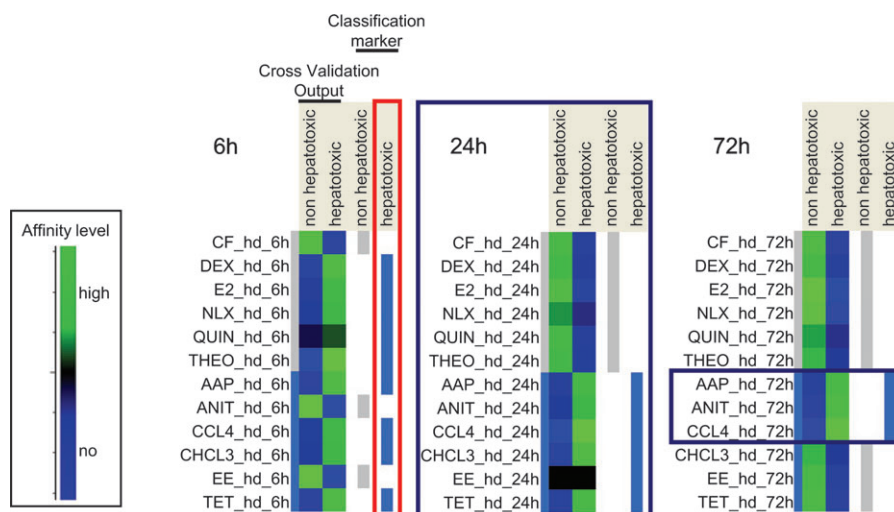


FIG. 2. Tile plots of 12 model compounds classified according to hepatotoxicity and nonhepatotoxicity 6, 24, and 72 h after hd treatment using leave-one-out cross-validation via SVM. Cross-validation output with an affinity level where the larger a value is, the higher is the affinity of the particular experiment toward the respective group (scale, green = high affinity) and the classification marker indicates the class (hepatotoxic [blue]/nonhepatotoxic [gray]) to which the compound was assigned.

discrimination between hepatotoxic and nonhepatotoxic model compounds 24 h after hd treatment (see “Discrimination Between Hepatotoxic and Nonhepatotoxic Compounds”). The best performance concerning the optimal gene set with a misclassification rate of 0% (with which to perform the classification) was reached with a classifier based on 64 genes. In Table 4 the top-scoring 64 genes are described.

Verification of Illumina Gene Expression Data with Quantitative Real-Time PCR

Quantitative real-time PCR was used to verify the Illumina microarray data collected in this study. For a direct comparison, liver RNA from the same animals as used for Illumina microarray hybridization was used. Mean expression ratios of all samples from identically treated animals (three biological replicates) versus time-matched vehicle controls were compared between Illumina microarray and TaqMan Low density array technology platforms.

In Figure 3, the gene expression changes of the 24-h samples from hd CCL4-treated rats are shown as an example and data from all 12 compounds summarized in parentheses in Table 4. The real-time PCR expression patterns of the 14 genes, chosen for verification, matched the expression patterns obtained from the Illumina microarray hybridization for all compounds confirming the Illumina gene expression results.

Verification of the Predictive Screening Test System by Two Unknown Compounds

The possibility that gene expression profiles could classify an UNC was tested using the aforementioned model compounds as a training set. Samples derived from rats acutely exposed to two UNC, A and B, for 24 h were taken for gene expression analysis on Illumina microarrays and then compared to the model previously described. UNC A was predicted to be hepatotoxic, UNC B as nonhepatotoxic (Fig. 4). As UNC A bromobenzene was used, an industrial chemical, which is known to cause hepatotoxicity by induction of liver necrosis (Heijne *et al.*, 2004; Lau and Monks, 1988). The histopathological findings of UNC A were scored and categorized (Table 2). Bromobenzene showed minimal liver damage at the ld level that increased to moderate liver cell necrosis with mild secondary effects after hd treatment. UNC B was an internal Merck KGaA compound, which did not show abnormal histopathological changes on day 1 (Table 2). According to the study design, UNC B was dosed daily for 14 days, and livers showed histopathological changes, including massive bridging liver necrosis with inflammatory bile duct lesions, only after 14 days.

DISCUSSION

The main focus of this study was to determine whether gene expression of a relatively small set of genes, known or suspected to be involved in hepatotoxicity, could discriminate

between known hepatotoxic and nonhepatotoxic compounds. The ultimate goal would be to establish a predictive system for acute hepatotoxicity. Twelve compounds were evaluated at 6, 24, and 72 h and the expression profiles of the six hepatotoxicants could be differentiated from the six nonhepatotoxicants. By using bioinformatic cross-validation approaches and gene ranking analysis, characteristic genes were extracted and functionally classified. Only samples after hd administration showed predictive results. Ld treatment showed no discriminative patterns, which correlated well with the histopathological observations in these animals.

Effects of Hepatotoxic Compounds

All six hepatotoxic compounds showed individual gene expression profiles, reflecting compound-specific differences at the molecular level (data not shown). After 24-h hd treatment only five genes were commonly deregulated by these hepatotoxicants. The xenobiotic metabolism enzyme *Fmo1* increases solubility and thereby ensures rapid excretion of xenobiotics (Eswaramoorthy *et al.*, 2006). Its downregulation may contribute to hepatotoxicity due to lack of elimination and emphasizes the importance of xenobiotic metabolism. The downregulation of *Maob*, which catalyzes the oxidative deamination of biogenic and neurobiogenic amines (Zhou *et al.*, 1995), further supports this. The differences in fold change levels of these commonly deregulated genes can also be a sign that different maximal toxic time points exist, for example, 6 h for CCL4 and 12 h for AAP (Minami *et al.*, 2005). The carbohydrate metabolism enzyme *Pygl*, was downregulated by all hepatotoxicants indicating a decrease in glycogenolysis, since it catalyzes the first step in glycogen degradation (Bollen *et al.*, 1998). This could indicate a lack of resourcing energy, correlating with depleted glycogen stores which is seen histopathologically. *Txnrd1* is involved in protecting cells from oxidative stress (Deroo *et al.*, 2004; Neumann *et al.*, 2003). Its upregulation indicates the generation of reactive oxygen species, potentially contributing to DNA and protein damage. *Txnrd1* is known to be upregulated by typical hepatotoxicants such as bromobenzene, thioacetamide, CCL4, and AAP (Minami *et al.*, 2005; Moto *et al.*, 2005) and is a sign of general cytotoxicity in the liver. *Abcb11* plays a major role in the hepatobiliary excretion of bile salts (Strautnieks *et al.*, 1998). Downregulation by hepatotoxicants could result in severe hepatic effects, including intrahepatic cholestasis (Hirano *et al.*, 2006) and hepatic steatosis (Figge *et al.*, 2004).

Discrimination of Hepatotoxicants and Nonhepatotoxicants

Some of the nonhepatotoxicants also showed unique profiles. For example, CF is well-known to cause hepatocarcinogenesis (Baldwin *et al.*, 1980; Corton *et al.*, 2000), however, in our short-term study CF was expected and shown to be nonhepatotoxic. At the gene expression level only typical PPAR- α -mediated responses were observed (Corton *et al.*, 2000; Richert *et al.*, 2003).

TABLE 4
Top-Scoring Gene Set with Fold Regulations (Illumina Microarray) Responsible for the Correct Discrimination between Hepatotoxic and Nonhepatotoxic Model Compounds 24 h after hd Treatment

Gene description	RefSeq	Symbol	Ranking	Hepatotoxic compounds						Nonhepatotoxic compounds					
				TET	CCL4	ANIT	EE	AAP	CHCL3	CF	THEO	NLX	E2	QUIN	DEX
Acute phase															
Lipopolysaccharide binding protein	NM_017208	<i>Lbp**</i>	16	8.2 (9.1)	3.7 (3.5)	13.1 (7.0)	16.6 (13.4)	2.1 (2.2)	4.5 (2.3)	-1.1* (-1.1)	4.3 (4.6)	1.6 (-1.2)	-1.0* (-1.7)	3.4 (2.4)	1.1* (-1.7)
Clusterin	NM_053021	<i>Clu</i>	30	1.2	1.8	1.3	1.0*	1.2	1.3	-1.1*	1.3	1.1*	-1.1*	1.1*	-1.4
Alpha(1)-inhibitor 3, variant I	NM_023103	<i>Mugl</i>	41	-1.3	-1.5	-1.5	-1.1*	-1.2	-1.3	1.1	-1.2	-1.2	-1.1*	1.0*	-1.2
Apoptosis															
Tumor necrosis factor receptor superfamily, member 1a	NM_013091	<i>Tnfrsf1a</i>	2	2.1	1.4	2.1	1.6	1.6*	1.3	-1.1*	1.1*	-1.2	1.0*	-1.2	-1.3
v-myc avian myelocytomatosis viral oncogene homolog	NM_012603	<i>Myc</i>	19	5.5	16.8	5.0	1.3	5.4	2.8*	1.2*	-1.6	1.5	-1.5*	-2.1	-1.8
Carbohydrate metabolism															
Liver glycogen phosphorylase	NM_022268	<i>Pygl**</i>	1	-3.5 (-4.8)	-3.2 (-3.5)	-3.1 (-4.6)	-2.5 (-4.9)	-3.2 (-4.6)	-1.8 (-4.4)	-1.4 (-1.4)	-1.3 (-1.4)	-1.4 (-2.2)	1.1* (1.2)	-1.2 (-1.4)	1.2 (-1.6)
Aldolase A	NM_012495	<i>Aldoa</i>	21	1.8	4.5	2.1	1.0*	1.9*	2.7	-1.6*	1.1*	-1.1*	1.1	1.2	1.5
Pyruvate kinase, liver and RBC	NM_012624	<i>Pklr</i>	38	-23.2	-7.2	-5.6	-13.3	-9.7	-4.7*	-3.6	-6.8	-4.4	1.2*	-2.7	-1.1*
Glucokinase	NM_012565	<i>Gck</i>	39	-1.1*	-3.4	-2.5	-5.2	-1.8*	2.0	-1.5*	2.1	-1.1*	1.1*	1.4*	1.6
Cell cycle progression															
Cyclin G1	NM_012923	<i>Ccng1</i>	62	3.6	14.5	1.9	1.0*	1.4*	2.6	-1.6	-1.1*	-1.0*	-1.0*	-1.1*	1.4
Cell survival and proliferation															
Insulin-like growth factor binding protein 1	NM_013144	<i>Igfbp1**</i>	4	101.3 (202.1)	40.0 (26.2)	10.5 (16.9)	6.9 (9.9)	26.1 (70.1)	4.6* (56.9)	10.7 (20.6)	-1.8* (1.2)	-1.0* (-2.1)	-1.7* (-1.5)	-2.0* (1.1)	1.8 (1.1)
Fibrinogen, beta polypeptide	NM_020071	<i>Fgb</i>	17	1.4	1.2	1.3	1.9	1.6	1.1*	1.2	1.2	-1.1*	-1.0*	1.2	-1.3
Ornithine decarboxylase 1	NM_012615	<i>Odc1</i>	18	3.4	3.7	2.2	-1.3*	1.8	2.5	-1.4	1.1*	1.1*	1.2	-1.2*	1.7
Lectin, galactose binding, soluble 3	NM_031832	<i>Lgals3</i>	43	3.8	21.6	3.0	3.4	1.0*	7.3	-1.6*	1.5	1.5	1.1*	1.4*	-1.1
Thioredoxin	NM_053800	<i>Txn</i>	47	1.1	1.7	1.4	-1.4*	1.6	2.2	-1.4	1.0*	1.3	1.2*	1.0*	1.0*
Tissue inhibitor of metalloproteinase 1	NM_053819	<i>Timp1**</i>	49	5.3 (11.0)	8.0 (7.5)	4.8 (6.0)	3.6 (6.9)	-1.7* (2.8)	7.7 (33.5)	-1.4* (-1.1)	2.1 (3.0)	1.6 (2.4)	1.3* (1.6)	2.1 (4.2)	1.6* (-1.3)
Prothymosin alpha	NM_021740	<i>Ptma</i>	60	1.9	3.0	1.9	1.0*	1.2*	2.3	1.1*	-1.6	-1.3	1.3	-1.5	-1.2*
Cell-cell signaling															
Fatty acid desaturase 1	NM_053445	<i>Fads1</i>	59	-12.6	-10.8	-1.0*	-1.7	-13.0	-1.7	-1.1*	-1.3*	1.0*	1.2*	1.3*	-3.3
Gap junction membrane channel protein beta 1	NM_017251	<i>Gjb1</i>	64	-1.2*	-4.4	-1.5	-1.1*	-1.3	-1.3	1.0*	-1.0*	-1.1*	1.1*	-1.0*	-1.3

Hepatocellular carcinoma																
S100 calcium-binding protein A9 (calgranulin B)	NM_053587	<i>S100a9**</i>	5	6.2 (14.3)	9.4 (7.6)	2.8 (3.2)	9.1 (17.3)	2.6 (56.5)	3.6 (12.0)	-1.6* (-1.1)	3.1* (2.8)	1.2* (1.1)	-1.1* (-1.2)	2.5 (1.5)	-2.1 (-7.0)	
	NM_022535	<i>Calu</i>	8	1.8	2.4	2.8	1.3	1.2	1.6	-1.4*	1.3	-1.4*	1.1*	1.1*	1.5	
Calumenin	NM_053822	<i>S100a8</i>	26	6.5	17.6	4.9	14.2	2.2*	13.4	-1.7*	2.1*	-1.2*	1.3*	1.1*	-1.6*	
Lipid metabolism																
ATP citrate lyase	NM_016987	<i>Acly**</i>	14	-5.7 (-9.0)	-3.5 (-4.8)	-4.0 (-4.4)	-3.2 (-4.7)	-8.4 (-9.9)	-3.2* (-3.9)	-3.6 (-5.8)	-2.2* (-1.1)	-2.2 (-2.5)	1.1* (1.6)	-2.2* (-1.3)	-1.5 (-2.8)	
Lipoprotein lipase	NM_012598	<i>Lpl</i>	25	3.1	6.9	2.1	2.8	-1.0*	4.1	1.9	1.3*	-1.9*	1.4	-1.1*	1.4*	
Acyl-CoA synthetase long-chain family member 1	NM_012820	<i>Acs1l</i>	28	-1.6	-3.6	-2.6	-1.1	-2.2	-1.7	-1.0*	1.0*	1.0*	1.1*	1.0*	-1.6	
Acetyl-coenzyme dehydrogenase, medium chain	ANM_016986	<i>Acadm</i>	52	-1.9	-3.1	-1.5	-2.0	-1.7	-1.2	1.3	-1.5	-1.1*	-1.0*	-1.4	-1.2	
Lipase, hepatic	NM_012597	<i>Lipc</i>	53	-2.8	-3.1	-1.4	-1.8	-2.8	-1.7	-1.6	-2.0	-1.4	1.0*	-1.4	-1.6	
Fatty acid synthase	NM_017332	<i>Fasn</i>	56	-32.8	-7.7	-3.0*	-13.6	-14.0	-2.4*	-6.3	-4.0*	-4.8	1.0*	-1.8*	1.5	
Fatty acid binding protein 1	NM_012556	<i>Fabp1</i>	63	-1.2	-1.4	-1.1	1.1	-1.4	-1.5	1.1*	1.1	-1.1*	1.1*	1.1*	-1.4	
Oxidative stress/DNA damage response																
Growth arrest and DNA damage-inducible 45 alpha	NM_024127	<i>Gadd45a**</i>	9	4.7 (6.8)	10.8 (12.9)	3.5 (3.0)	1.7 (2.1)	2.6* (4.4)	1.8 (4.0)	-1.5* (-1.6)	-1.3* (-1.1)	1.5 (-1.1)	-1.2* (-1.1)	1.1* (-1.1)	-1.9 (-3.3)	
Apurinic/apyrimidinic endonuclease 1	NM_024148	<i>Apex1</i>	32	2.1	3.1	1.6	-1.6	1.9*	2.1	-1.4	-1.4	-1.2	1.6	-1.2*	-1.0*	
Tumor protein p53	NM_030989	<i>Tp53</i>	33	2.4	2.3	1.1	-1.3	1.0*	1.6	-1.1*	-1.1	-1.5	1.4	-1.3	-1.1	
B-cell translocation gene 2, anti-proliferative	NM_017259	<i>Btg2</i>	42	4.7	4.1	4.0	2.0	-1.1*	2.4	1.9*	-1.2*	-1.0*	1.1*	-1.0*	-1.2*	
DNA damage-inducible transcript 3	NM_024134	<i>Ddit3</i>	54	10.0	10.9	1.5	1.1	2.0	2.2	-1.2*	1.1*	-1.4*	1.7	-1.2*	-1.0*	
Oxidative stress/protein damage response																
Cathepsin L	NM_013156	<i>Ctsl</i>	10	3.2	3.5	2.1	1.2	1.6	2.2	1.1*	-1.2	1.3	1.0*	1.1*	1.3	
Serine protease inhibitor	NM_012657	<i>Spin2b</i>	11	-4.3	-3.6	-1.3	-1.9	-1.9	-2.5	1.3	-1.4	-1.1	1.2	-1.0*	-1.0*	
Heat shock 70-kDa protein 1A	NM_031971	<i>Hspa1a</i>	24	5.3	25.5	8.0	-1.1*	18.3	14.3	-1.7*	1.5*	1.1*	1.1*	-1.2*	1.7	
Oxidative stress																
Catalase	NM_012520	<i>Car**</i>	35	-4.1 (-3.0)	-5.6 (-5.0)	-2.1 (-2.6)	-1.4 (-2.3)	-1.7 (-3.3)	-1.3 (-2.4)	1.0* (-1.1)	-1.3* (-1.1)	1.2 (-1.0)	-1.2 (-1.0)	1.0* (-1.9)	-2.4 (-4.8)	
Glutathione peroxidase 1	NM_030826	<i>Gpx1</i>	55	-1.8	-2.2	-1.4	-1.9	-4.0	-1.9	-1.2	-1.7	-1.1*	-1.0*	-1.1*	-2.0	
Regeneration																
Fibrinogen, alpha polypeptide	NM_001008724	<i>Fga</i>	13	2.4	-1.0*	4.7	4.3	1.9	1.4	1.0*	1.2	-1.1*	-1.1*	1.6	-1.6*	
Signal transduction/transcription factor																
Signal transducer and activator of transcription 3	NM_012747	<i>Stat3**</i>	22	5.5 (5.7)	2.4 (1.4)	3.0 (3.0)	3.8 (4.0)	2.3 (1.1)	1.2* (2.9)	1.5* (1.4)	1.5* (1.4)	1.4* (-1.1)	-1.1* (-1.1)	1.2* (1.7)	1.2* (-1.5)	

TABLE 4—Continued

Gene description	RefSeq	Symbol	Ranking	Hepatotoxic compounds						Nonhepatotoxic compounds					
				TET	CCL4	ANIT	EE	AAP	CHCL3	CF	THEO	NLX	E2	QUIN	DEX
Membrane interacting protein of RGS16	NM_032615	<i>Mir16</i>	37	1.5	3.2	2.2	1.3	2.1	1.5	1.1*	1.2*	1.7	-1.1*	1.1*	-2.3
Sterol regulatory element binding factor 1	XM_213329	<i>Srebf1</i>	40	-1.6	-6.9	-7.2	-4.0	-7.7	-1.1*	-2.1	-2.6	-1.7	1.1*	-1.1*	-1.3*
I-kappa-B-beta	NM_030867	<i>Nfkbib</i>	45	1.5	2.8	2.2	-1.2	1.2	1.6	-1.1*	1.0*	-1.0*	1.2	-1.1*	-1.0*
Tissue organization															
Keratin complex 1, acidic, gene 18	NM_053976	<i>Krt1-18</i>	3	1.9	1.9	2.9	1.5	1.3*	2.8	-1.6	1.3*	1.1*	1.1*	-1.2*	-1.0*
Keratin complex 2, basic, gene 8	NM_199370	<i>Krt2-8</i>	7	1.7	2.6	2.6	1.0*	1.2*	3.7	-1.5	1.5	1.1*	-1.3	-1.1*	-1.3
Intercellular adhesion molecule 1	NM_012967	<i>Icam1</i>	12	1.6	1.6	1.7	1.1*	-1.6*	1.9	-3.1	-1.4*	-1.2*	-1.2*	-1.2*	-1.5
Carcinoembryonic antigen-related cell adhesion molecule 1	NM_031755	<i>Ceacam1</i>	50	1.0*	-2.7	-1.4*	-1.7	-1.5	1.0*	1.1*	-1.5	1.1*	1.0*	1.5	1.1
Urea cycle															
Ornithine transcarbamylase	NM_013078	<i>Otc**</i>	29	-4.1 (-4.2)	-7.8 (-24.4)	-1.7 (-2.5)-2.0 (-3.1)	-2.7 (-7.7)	-1.8 (-5.2)	-1.1* (-1.1)-1.5 (-1.2)	-1.1 (-1.6)	-1.1* (1.3)	-1.2 (-1.4)	-1.6 (-3.5)		
Argininosuccinate lyase	NM_021577	<i>Asl</i>	51	2.6	2.0	1.4	1.0*	1.4*	2.6	1.0*	-1.3	1.1*	-1.0*	1.1*	1.1*
Xenobiotic metabolism/Phase 1															
Monoamine oxidase B	NM_013198	<i>Maob</i>	6	-1.6	-3.2	-1.7	-1.9	-1.8	-1.6	-1.1*	1.0*	1.0*	-1.1*	-1.2	-1.1
Cytochrome P450, subfamily IID3	NM_173093	<i>Cyp2d3</i>	15	-3.1	-3.8	-1.3	-2.0	-1.5	-1.3	1.1*	-1.1	1.2*	1.1	-1.1*	-1.1*
3-Hydroxyisobutyrate dehydrogenase	NM_022243	<i>Hibadh</i>	23	-1.8	-3.0	-1.5	-1.3	-1.7	-1.1	1.1*	-1.3	1.1*	-1.2	1.1	1.1
Aldehyde dehydrogenase family 3, subfamily A2	NM_031731	<i>Aldh3a2</i>	31	-2.3	-3.4	-1.3*	-2.0	-1.6	-1.2	-1.2*	-1.1*	1.0*	-1.0*	-1.2*	-1.1*
Flavin containing monooxygenase 1	NM_012792	<i>Fmo1**</i>	34	-2.9 (-23.5)	-10.7 (-1062.8)	-3.9 (-7.5)-2.0 (-1.5)	-4.7 (-32.0)	-4.8 (-77.6)	1.0* (2.1)	-1.7* (-1.2)	-1.2* (-1.8)	-1.1* (-1.1)	-1.4* (-1.0)	-1.1* (-2.5)	
Diaphorase 1	NM_138877	<i>Dial</i>	48	-2.8	-3.1	-2.1	-2.8	-1.8	-1.5*	-1.6	1.0*	1.6*	-1.1*	-1.2	-1.8
Xenobiotic metabolism/Phase 2															
Glutathione S-transferase, mu type 3 (Yb3)	NM_031154	<i>Gstm3**</i>	46	-12.7 (-11.0)	-33.1 (-62.9)	-2.2 (-3.0)-3.3 (-5.0)	-4.4 (-14.5)	-2.6 (-6.4)	-1.1* (-1.2)	-1.8 (-1.0)	-1.3 (-2.6)	-1.3 (-1.6)	-1.3 (1.2)	-2.2 (-3.7)	
Xenobiotic metabolism/Phase 3															
Solute carrier family 2, member 1	NM_138827	<i>Slc2a1</i>	20	1.8	6.9	2.2	1.4*	1.7	2.5	-1.3*	-1.4*	1.4*	-1.4*	-1.2*	1.1*
ATP-binding cassette, sub-family B (MDR/TAP), member 1	NM_012623	<i>Abcb1**</i>	27	34.2 (83.6)	107.4 (299.6)	4.2 (9.8)	3.3 (6.3)	10.4 (40.3)	47.8 (1738.3)	2.0* (2.6)	1.1* (1.8)	4.3 (26.0)	-2.0* (1.0)	1.5* (2.2)	-1.2* (-7.0)

ATP-binding cassette, subfamily C (CFTR/MRP), member 3	NM_080581	<i>Abcc3</i>	36	3.3	1.7	2.2	1.4	15.7	6.7	-1.7*	-1.6*	3.5	1.0*	-1.7*	-1.7
Solute carrier family 21, member 10	NM_031650	<i>Slc21a10</i>	58	-1.5	-5.8	-2.2	-1.8	-3.3	-1.5*	-1.2	1.1	1.1*	-1.0*	1.1*	1.0*
Others															
Transthyretin	NM_012681	<i>Ttr</i>	44	-1.2	-2.9	-1.3	-1.2	-1.6	-1.1	1.0*	-1.0*	-1.2*	1.2	-1.0*	-1.2
Poliovirus receptor	NM_017076	<i>PVR</i>	57	3.1	22.4	4.0	1.2*	-1.1*	4.5	-1.4*	-1.3*	-1.0*	1.1*	1.3*	-1.1*
Thyroid hormone responsive protein	NM_012703	<i>Thrsp</i>	61	-21.2	-17.7	-2.6	-6.0	-20.2	-2.3	-4.2	-4.5	-3.3	-1.3*	-1.0*	1.2*

Note. Genes taken for verification with RT-PCR are marked with “***” alongside the gene symbol and their respective fold regulations are placed in parenthesis. Not significant fold regulations are marked with “*”.

A subset of genes was defined that allowed an accurate prediction of hepatotoxicity. This was seen in particular 24 h after hd treatment, reflecting the time point where most pronounced and characteristic deregulations occurred. At 6 h the high misclassification rate (58.3%) can probably be attributed to early stress responses caused by intraperitoneal dosing, immune responses, and animal handling. At 72 h, the model correctly classified only three of the hepatotoxic compounds. This may be an indication of the regeneration effects that have occurred after a single treatment (Mehendale, 2005). The PCA showed that most compounds moved toward the main cluster, suggesting similar gene expression profiles. This is probably due to effective removal of the substance via metabolism and excretion, allowing the liver to recover. The three compounds, AAP, ANIT, and CCL4, predicted to be hepatotoxic after 72 h, reinforces the severity of hepatotoxicity of these compounds. Their distinct lasting effects on gene expression correlated very well with the histopathological findings taken at 72 h (only these three compounds showed changes). Interestingly, ANIT was predicted to be hepatotoxic only after 24 and 72 h and at 6 h was predicted to be nonhepatotoxic. This is consistent with the publication of Orsler *et al.* (1999) who showed that histopathological changes after administration of ANIT to rats were observed only after 10–15 h. AAP was correctly predicted to be hepatotoxic at all time points, which emphasizes the fact that AAP is a potent, acute hepatotoxicant. This study is in concordance with Huang *et al.* (2004), who demonstrated that a dose of 4500 mg/kg AAP induced a distinct gene expression profile, which related directly to its hepatotoxicity.

The most distinct gene expression changes were observed after CCL4 exposure. This corresponds very well with the severe liver cell damage with secondary inflammation and regenerative/proliferation effects, which was seen histopathologically. The data support the fact that the estimated maximal toxic time point, based on gene expression profiles, was 6 h (Minami *et al.*, 2005).

General Comments to the Predictive Test System for Hepatotoxicants

It is worth noting that to establish this screening system, outbred rats were used to deliberately reflect the biological variance of animals within a certain range of genetic polymorphisms. This reflects better the normal human situation. Furthermore, the predictive test system demonstrated a certain robustness since the discrimination between hepatotoxic and nonhepatotoxic compounds was possible regardless of the different hepatotoxic characteristics (cholestasis, steatosis, or necrosis). The use of leave-one-out cross-validation on the one hand and the consideration that the data set of a model compound is composed of biological replicates (technical replicates were condensed) on the other hand indicate a robust test system, suggesting a potential application in the prediction of untested compounds.

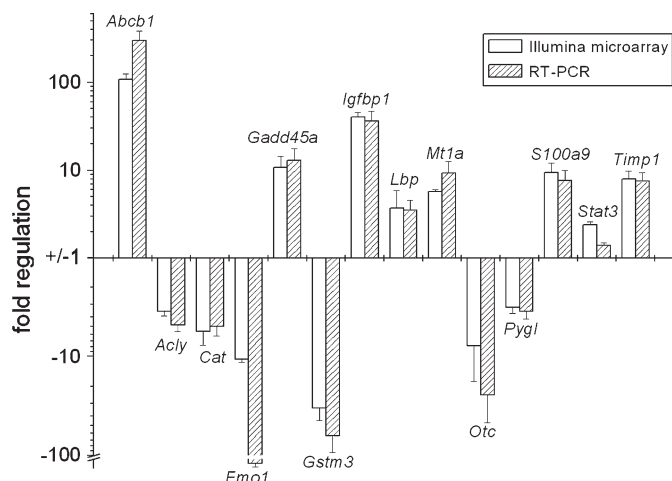


FIG. 3. Expression pattern of 14 genes determined by Illumina microarray (first column) and RT-PCR (second column) 24 h after CCL4 hd treatment. Genes are described in Table 3.

Top-Scoring Genes for Class Prediction after 24 h

Twenty-four hours after hd treatment the best discrimination between hepatotoxicants and nonhepatotoxicants was achieved by the leave-one-out cross-validation method. Sixty-four genes (Table 4) were found to be responsible for this class prediction and reflected typical hepatotoxicity responses. The rank order is characterized by genes with different biological function/toxicological relevance. The top-scored gene *Pygl* was significantly downregulated only by hepatotoxicants corroborating the suggestion that *Pygl* could be an appropriate hepatotoxicity safety marker. The second highest scoring gene, tumor necrosis factor receptor superfamily member 1a (*Tnfrsf1a*), plays an important role in apoptosis by mediating *TNF- α* signaling, whose overexpression in acute disease states can lead to liver injury (Mohammed *et al.*, 2004; Volpes *et al.*, 1992; Yamada *et al.*, 1998). Keratin complex 1 acidic gene 18 (*Krt1-18*) forms intermediate filaments in liver (Oshima *et al.*, 1996). Disruption or absence of keratins in the liver can lead to mild hepatitis and increased sensitivity to hepatotoxins (Baribault *et al.*, 1994; Ku *et al.*, 1996). Caulin *et al.* (2000) found that increases in *Krt1-18* can resist *TNF*-induced apoptosis, suggesting *Krt1-18* is involved in liver regeneration.

In general, the top-scoring genes showed the most pronounced deregulation in many biological categories, such as Phases 1 and 2 xenobiotic metabolism, lipid metabolism, and cell proliferation. Disturbances in lipid metabolism occurred by downregulation of genes such as ATP citrate lyase (*Acly*), which has an important role in supplying acetyl-CoA for both cholesterologenesis and lipogenesis (Pearce *et al.*, 1998). Therefore, the lipid biosynthesis level in the liver is low, suggesting low energy resources which may contribute to the pathogenesis of liver damage (Beigneux *et al.*, 2004). The DNA damage response gene, *Gadd45a* is typically upregulated by hepato-

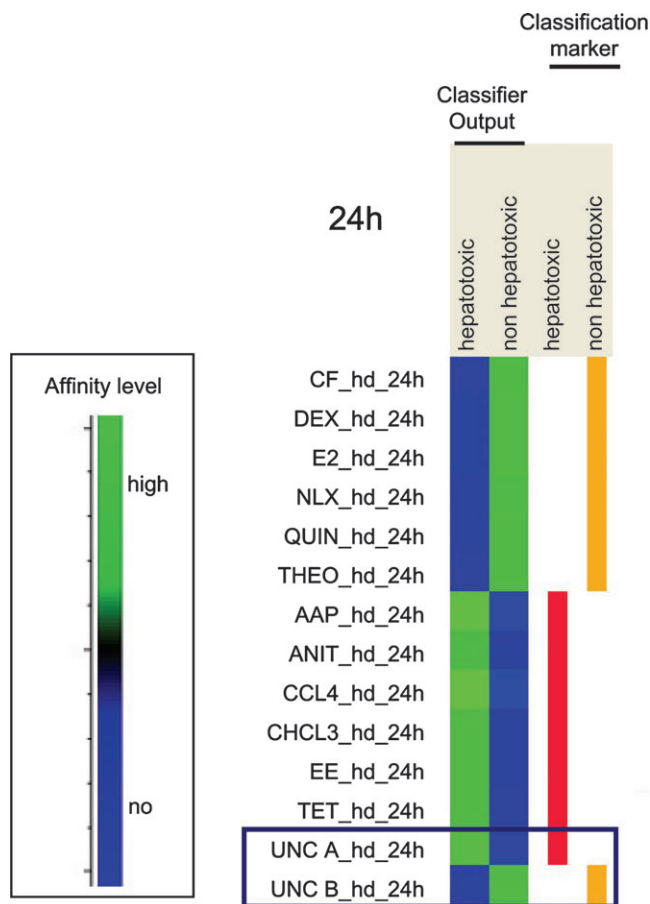


FIG. 4. Classification analysis tile plot of the prediction of two UNC compounds, A and B, according to hepatotoxicity and nonhepatotoxicity 24 h after hd treatment based on a training set precomputed by 12 model compounds. UNC A was predicted to be hepatotoxic, UNC B as nonhepatotoxic. Classifier output with an affinity level where the larger a value is, the higher is the affinity of the two UNC compounds toward the respective group (scale, green = high affinity) and the classification marker indicates the class (hepatotoxic [red]/nonhepatotoxic [orange]) to which the two UNC compounds were assigned.

toxicants (Bartosiewicz *et al.*, 2001), which is in concordance with our data. The insulin-like growth factor binding protein 1 (*Igfbp1*) modulates insulin-like growth factor, which plays an essential role in the regulation of metabolism, growth, and development. *Igfbp1* has been shown previously to be upregulated after acute liver injury (Scharf *et al.*, 2004), again confirming the relevance of our highest ranked genes.

Prediction of Two UNC compounds

The model created was used to predict the hepatotoxicity of two UNC compounds. UNC A was predicted to be hepatotoxic, which correlated well with the histopathological findings, a good prevalidation of our test system. The second UNC, UNC B, was predicted to be nonhepatotoxic, which correlated well with the lack of histopathological changes observed at 24 h. Classification analysis based on our 24-h model was able to predict UNC

B to be hepatotoxic after 14 days of daily dosing (data not shown). This indicates that gene expression was affected by the compound after repeated dosage but not by a single dose.

In conclusion, we have presented evidence that the accurate discrimination between acute hepatotoxic compounds and non-hepatotoxicants, based on their gene expression profiles was possible 24-h postadministration. A prevalidation with two UNC's showed that the model we created was able to predict acute hepatotoxicants. The use of this model for more chronic, repeat-dose toxicity is still unclear. Preliminary data from UNC B suggest that the model can predict hepatotoxicity at 2 weeks. Therefore, further work is needed to elucidate hepatotoxicity signatures for other endpoints (e.g., repeated dose, other organ toxicity, and other species) and time points. Regarding the relatively small set of genes we conclude that focused gene microarrays are sufficient to classify compounds with respect to acute hepatotoxicity.

SUPPLEMENTARY DATA

Supplementary data are available online at <http://toxsci.oxfordjournals.org/>.

ACKNOWLEDGMENTS

The authors wish to thank Dr Anja von Heydebreck (Bio&Chemoinformatics, Merck KGaA) for her bioinformatics support and Dr Stefan O. Müller (Molecular Toxicology, Institute of Toxicology, Merck KGaA) for his comments and helpful discussion.

REFERENCES

- Amacher, D. E., and Martin, B. A. (1997). Tetracycline-induced steatosis in primary canine hepatocyte cultures. *Fundam. Appl. Toxicol.* **40**, 256–263.
- Baldwin, J. R., Witiak, D. T., and Feller, D. R. (1980). Disposition of clofibrate in the rat. Acute and chronic administration. *Biochem. Pharmacol.* **29**, 3143–3154.
- Baribault, H., Penner, J., Iozzo, R. V., and Wilson-Heiner, M. (1994). Colorectal hyperplasia and inflammation in keratin 8-deficient FVB/N mice. *Genes Dev.* **8**, 2964–2973.
- Bartosiewicz, M. J., Jenkins, D., Penn, S., Emery, J., and Buckpitt, A. (2001). Unique gene expression patterns in liver and kidney associated with exposure to chemical toxicants. *J. Pharmacol. Exp. Ther.* **297**, 895–905.
- Beigneux, A. P., Kosinski, C., Gavino, B., Horton, J. D., Skarnes, W. C., and Young, S. G. (2004). ATP-citrate lyase deficiency in the mouse. *J. Biol. Chem.* **279**, 9557–9564.
- Bollen, M., Keppens, S., and Stalmans, W. (1998). Specific features of glycogen metabolism in the liver. *Biochem. J.* **336**(Pt 1), 19–31.
- Brattin, W. J., Glende, E. A., Jr, and Recknagel, R. O. (1985). Pathological mechanisms in carbon tetrachloride hepatotoxicity. *J. Free Radic. Biol. Med.* **1**, 27–38.
- Caulin, C., Ware, C. F., Magin, T. M., and Oshima, R. G. (2000). Keratin-dependent, epithelial resistance to tumor necrosis factor-induced apoptosis. *J. Cell Biol.* **149**, 17–22.
- Corton, J. C., Anderson, S. P., and Stauber, A. (2000). Central role of peroxisome proliferator-activated receptors in the actions of peroxisome proliferators. *Annu. Rev. Pharmacol. Toxicol.* **40**, 491–518.
- de Longueville, F., Atienzar, F. A., Marcq, L., Dufrane, S., Evrard, S., Wouters, L., Leroux, F., Bertholet, V., Gerin, B., Whomsley, R., *et al.* (2003). Use of a low-density microarray for studying gene expression patterns induced by hepatotoxicants on primary cultures of rat hepatocytes. *Toxicol. Sci.* **75**, 378–392.
- Deroo, B. J., Hewitt, S. C., Peddada, S. D., and Korach, K. S. (2004). Estradiol regulates the thioredoxin antioxidant system in the mouse uterus. *Endocrinology* **145**, 5485–5492.
- Duggan, D. J., Bittner, M., Chen, Y., Meltzer, P., and Trent, J. M. (1999). Expression profiling using cDNA microarrays. *Nat. Genet.* **21**, 10–14.
- Eberwine, J., Yeh, H., Miyashiro, K., Cao, Y., Nair, S., Finnell, R., Zettel, M., and Coleman, P. (1992). Analysis of gene expression in single live neurons. *Proc. Natl. Acad. Sci. U. S. A.* **89**, 3010–3014.
- Eswaramoorthy, S., Bonanno, J. B., Burley, S. K., and Swaminathan, S. (2006). Mechanism of action of a flavin-containing monooxygenase. *Proc. Natl. Acad. Sci. U. S. A.* **103**, 9832–9837.
- Figge, A., Lammert, F., Paigen, B., Henkel, A., Matern, S., Korstanje, R., Shneider, B. L., Chen, F., Stoltenberg, E., Spatz, K., *et al.* (2004). Hepatic overexpression of murine Abcb11 increases hepatobiliary lipid secretion and reduces hepatic steatosis. *J. Biol. Chem.* **279**, 2790–2799.
- Fromenty, B., and Pessayre, D. (1995). Inhibition of mitochondrial beta-oxidation as a mechanism of hepatotoxicity. *Pharmacol. Ther.* **67**, 101–154.
- Galinsky, V. L. (2003). Automatic registration of microarray images. I. Rectangular grid. *Bioinformatics* **19**, 1824–1831.
- Garcia Monzon, C., Noguerado, A., Hidalgo, S., and Escudero, V. (1985). [Cholestatic hepatitis caused by erythromycin estolate]. *Rev. Clin. Esp.* **177**, 420–421.
- Gunderson, K. L., Kruglyak, S., Graige, M. S., Garcia, F., Kermani, B. G., Zhao, C., Che, D., Dickinson, T., Wickham, E., Bierle, J., *et al.* (2004). Decoding randomly ordered DNA arrays. *Genome Res.* **14**, 870–877.
- Hamadeh, H. K., Bushel, P. R., Jayadev, S., Martin, K., DiSorbo, O., Sieber, S., Bennett, L., Tennant, R., Stoll, R., Barrett, J. C., *et al.* (2002). Gene expression analysis reveals chemical-specific profiles. *Toxicol. Sci.* **67**, 219–231.
- Heijne, W. H., Slitt, A. L., van Bladeren, P. J., Groten, J. P., Klaassen, C. D., Stierum, R. H., and van Ommen, B. (2004). Bromobenzene-induced hepatotoxicity at the transcriptome level. *Toxicol. Sci.* **79**, 411–422.
- Hirano, H., Kurata, A., Onishi, Y., Sakurai, A., Saito, H., Nakagawa, H., Nagakura, M., Tarui, S., Kanamori, Y., Kitajima, M., *et al.* (2006). High-speed screening and QSAR analysis of human ATP-binding cassette transporter ABCB11 (bile salt export pump) to predict drug-induced intrahepatic cholestasis. *Mol. Pharm.* **3**, 252–265.
- Huang, Q., Jin, X., Gaillard, E. T., Knight, B. L., Pack, F. D., Stoltz, J. H., Jayadev, S., and Blanchard, K. T. (2004). Gene expression profiling reveals multiple toxicity endpoints induced by hepatotoxicants. *Mutat. Res.* **549**, 147–167.
- James, L. P., Mayeux, P. R., and Hinson, J. A. (2003). Acetaminophen-induced hepatotoxicity. *Drug Metab. Dispos.* **31**, 1499–1506.
- Krell, H., Hoke, H., and Pfaff, E. (1982). Development of intrahepatic cholestasis by alpha-naphthylisothiocyanate in rats. *Gastroenterology* **82**, 507–514.
- Ku, N. O., Michie, S. A., Soetikno, R. M., Resurreccion, E. Z., Broome, R. L., Oshima, R. G., and Omary, M. B. (1996). Susceptibility to hepatotoxicity in transgenic mice that express a dominant-negative human keratin 18 mutant. *J. Clin. Invest.* **98**, 1034–1046.
- Kuhn, K., Baker, S. C., Chudin, E., Lieu, M. H., Oeser, S., Bennett, H., Rigault, P., Barker, D., McDaniel, T. K., and Chee, M. S. (2004). A novel, high-

- performance random array platform for quantitative gene expression profiling. *Genome Res.* **14**, 2347–2356.
- Lau, S. S., and Monks, T. J. (1988). The contribution of bromobenzene to our current understanding of chemically-induced toxicities. *Life Sci.* **42**, 1259–1269.
- Maggioli, J., Hoover, A., and Weng, L. (2006). Toxicogenomic analysis methods for predictive toxicology. *J. Pharmacol. Toxicol. Methods* **53**, 31–37.
- Mehendale, H. M. (2005). Tissue repair: An important determinant of final outcome of toxicant-induced injury. *Toxicol. Pathol.* **33**, 41–51.
- Mehendale, H. M., Roth, R. A., Gandolfi, A. J., Klaunig, J. E., Lemasters, J. J., and Curtis, L. R. (1994). Novel mechanisms in chemically induced hepatotoxicity. *FASEB J.* **8**, 1285–1295.
- Minami, K., Saito, T., Narahara, M., Tomita, H., Kato, H., Sugiyama, H., Katoh, M., Nakajima, M., and Yokoi, T. (2005). Relationship between hepatic gene expression profiles and hepatotoxicity in five typical hepatotoxicant-administered rats. *Toxicol. Sci.* **87**, 296–305.
- Mohammed, F. F., Smookler, D. S., Taylor, S. E., Fingleton, B., Kassiri, Z., Sanchez, O. H., English, J. L., Matrisian, L. M., Au, B., Yeh, W. C., et al. (2004). Abnormal TNF activity in Timp3^{-/-} mice leads to chronic hepatic inflammation and failure of liver regeneration. *Nat. Genet.* **36**, 969–977.
- Moto, M., Okamura, M., Muto, T., Kashida, Y., Machida, N., and Mistumori, K. (2005). Molecular pathological analysis on the mechanism of liver carcinogenesis in dicyclanil-treated mice. *Toxicology* **207**, 419–436.
- Neumann, C. A., Krause, D. S., Carman, C. V., Das, S., Dubey, D. P., Abraham, J. L., Bronson, R. T., Fujiwara, Y., Orkin, S. H., and Van Etten, R. A. (2003). Essential role for the peroxiredoxin Prdx1 in erythrocyte antioxidant defence and tumour suppression. *Nature* **424**, 561–565.
- Orsler, D. J., Ahmed-Choudhury, J., Chipman, J. K., Hammond, T., and Coleman, R. (1999). ANIT-induced disruption of biliary function in rat hepatocyte couplets. *Toxicol. Sci.* **47**, 203–210.
- Oshima, R. G., Baribault, H., and Caulin, C. (1996). Oncogenic regulation and function of keratins 8 and 18. *Cancer Metastasis Rev.* **15**, 445–471.
- Pearce, N. J., Yates, J. W., Berkhout, T. A., Jackson, B., Tew, D., Boyd, H., Camilleri, P., Sweeney, P., Gribble, A. D., Shaw, A., et al. (1998). The role of ATP citrate-lyase in the metabolic regulation of plasma lipids. Hypolipidaemic effects of SB-204990, a lactone prodrug of the potent ATP citrate-lyase inhibitor SB-201076. *Biochem. J.* **334**(Pt 1), 113–119.
- Prescott, L. F. (1980). Hepatotoxicity of mild analgesics. *Br. J. Clin. Pharmacol.* **10**(Suppl. 2), 373S–379S.
- Richert, L., Lamboley, C., Viollon-Abadie, C., Grass, P., Hartmann, N., Laurent, S., Heyd, B., Manton, G., Chibout, S. D., and Staedtler, F. (2003). Effects of clofibric acid on mRNA expression profiles in primary cultures of rat, mouse and human hepatocytes. *Toxicol. Appl. Pharmacol.* **191**, 130–146.
- Scharf, J. G., Dombrowski, F., Novosyadlyy, R., Eisenbach, C., Demori, I., Kubler, B., and Braulke, T. (2004). Insulin-like growth factor (IGF)-binding protein-1 is highly induced during acute carbon tetrachloride liver injury and potentiates the IGF-I-stimulated activation of rat hepatic stellate cells. *Endocrinology* **145**, 3463–3472.
- Schena, M., Shalon, D., Davis, R. W., and Brown, P. O. (1995). Quantitative monitoring of gene expression patterns with a complementary DNA microarray. *Science* **270**, 467–470.
- Stemmers, F. J., and Gunderson, K. L. (2005). Illumina, Inc. *Pharmacogenomics* **6**, 777–782.
- Steiner, G., Suter, L., Boess, F., Gasser, R., de Vera, M. C., Albertini, S., and Ruepp, S. (2004). Discriminating different classes of toxicants by transcript profiling. *Environ. Health Perspect.* **112**, 1236–1248.
- Strautnieks, S. S., Bull, L. N., Knisely, A. S., Kocoshis, S. A., Dahl, N., Arnell, H., Sokal, E., Dahan, K., Childs, S., Ling, V., et al. (1998). A gene encoding a liver-specific ABC transporter is mutated in progressive familial intrahepatic cholestasis. *Nat. Genet.* **20**, 233–238.
- Thomas, R. S., Rank, D. R., Penn, S. G., Zastrow, G. M., Hayes, K. R., Pande, K., Glover, E., Silander, T., Craven, M. W., Reddy, J. K., et al. (2001). Identification of toxicologically predictive gene sets using cDNA microarrays. *Mol. Pharmacol.* **60**, 1189–1194.
- Tuschl, G., and Mueller, S. O. (2006). Effects of cell culture conditions on primary rat hepatocytes-cell morphology and differential gene expression. *Toxicology* **218**, 205–215.
- Ulrich, R., and Friend, S. H. (2002). Toxicogenomics and drug discovery: Will new technologies help us produce better drugs? *Nat. Rev. Drug Discov.* **1**, 84–88.
- Venkateswaran, S., Pari, L., and Viswanathan, P. (1998). Antiperoxidative effect of Livex, a herbal formulation against erythromycin estolate induced lipid peroxidation in rats. *Phytother. Res.* **12**, 1148–1171.
- Volpes, R., van den Oord, J. J., De Vos, R., and Desmet, V. J. (1992). Hepatic expression of type A and type B receptors for tumor necrosis factor. *J. Hepatol.* **14**, 361–369.
- Wang, P. Y., Kaneko, T., Tsukada, H., Nakano, M., Nakajima, T., and Sato, A. (1997). Time courses of hepatic injuries induced by chloroform and by carbon tetrachloride: Comparison of biochemical and histopathological changes. *Arch. Toxicol.* **71**, 638–645.
- Waring, J. F., Jolly, R. A., Ciurlionis, R., Lum, P. Y., Praetstgaard, J. T., Morfitt, D. C., Buratto, B., Roberts, C., Schadt, E., and Ulrich, R. G. (2001). Clustering of hepatotoxins based on mechanism of toxicity using gene expression profiles. *Toxicol. Appl. Pharmacol.* **175**, 28–42.
- Weber, L. W., Boll, M., and Stampfl, A. (2003). Hepatotoxicity and mechanism of action of haloalkanes: Carbon tetrachloride as a toxicological model. *Crit. Rev. Toxicol.* **33**, 105–136.
- Yadete, F., Laegreid, A., Bakke, I., Kusnierczyk, W., Komorowski, J., Waldum, H. L., and Sandvik, A. K. (2003). Liver gene expression in rats in response to the peroxisome proliferator-activated receptor- α agonist ciprofibrate. *Physiol. Genomics* **15**, 9–19.
- Yamada, Y., Webber, E. M., Kirillova, I., Peschon, J. J., and Fausto, N. (1998). Analysis of liver regeneration in mice lacking type 1 or type 2 tumor necrosis factor receptor: Requirement for type 1 but not type 2 receptor. *Hepatology* **28**, 959–970.
- Yamamoto, T., Kikkawa, R., Yamada, H., and Horii, I. (2006). Investigation of proteomic biomarkers in vivo hepatotoxicity study of rat liver: Toxicity differentiation in hepatotoxicants. *J. Toxicol. Sci.* **31**, 49–60.
- Zhou, B. P., Lewis, D. A., Kwan, S. W., and Abell, C. W. (1995). Flavinoylation of monoamine oxidase B. *J. Biol. Chem.* **270**, 23653–23660.